THE JOURNAL OF BIOLOGICAL CHEMISTRY VOL. 283, NO. 36, pp. 25014–25026, September 5, 2008

Palmitoylation and Membrane Interactions of the Neuroprotective Chaperone Cysteine-string Protein*[S]

Received for publication, March 18, 2008, and in revised form, July 1, 2008 Published, JBC Papers in Press, July 2, 2008, DOI 10.1074/jbc.M802140200

Jennifer Greaves[‡], Christine Salaun[§], Yuko Fukata[¶‖], Masaki Fukata[¶‖], and Luke H. Chamberlain[‡1]

From the [‡]Centre for Integrative Physiology, School of Biomedical Sciences, Hugh Robson Building, University of Edinburgh, Edinburgh EH8 9XD, United Kingdom, the [§]Faculte de Medecine Paris Descartes, Site Necker, INSERM U845, 156 Rue de Vaugirard, Paris 75730 cedex 15, France, the [¶]Division of Membrane Physiology, National Institute for Physiological Sciences, 5-1 Higashiyama, Myodaiji, Okazaki 444-8787, Japan, and [‖]Precursory Research for Embryonic Science and Technology, Japan Science and Technology Agency, 3-5 Chiyoda, Tokyo 102-0075, Japan

Cysteine-string protein (CSP) is an extensively palmitoylated DnaJ-family chaperone, which exerts an important neuroprotective function. Palmitoylation is required for the intracellular sorting and function of CSP, and thus it is important to understand how this essential modification of CSP is regulated. Recent work identified 23 putative palmitoyl transferases containing a conserved DHHC domain in mammalian cells, and here we show that palmitoylation of CSP is enhanced specifically by co-expression of the Golgi-localized palmitoyl transferases DHHC3, DHHC7, DHHC15, or DHHC17. Indeed, these DHHC proteins promote stable membrane attachment of CSP, which is otherwise cytosolic. An inverse correlation was identified between membrane affinity of unpalmitoylated CSP mutants and subsequent palmitoylation: mutants with an increased membrane affinity localize to the endoplasmic reticulum (ER) and are physically separated from the Golgi-localized DHHC proteins. Palmitoylation of an ER-localized mutant could be rescued by brefeldin A treatment, which promotes the mixing of ER and Golgi membranes. Interestingly though, the palmitoylated mutant remained at the ER following brefeldin A washout and did not traffic to more distal membrane compartments. We propose that CSP has a weak membrane affinity that allows the protein to locate its partner Golgi-localized DHHC proteins directly by membrane "sampling." Mutations that enhance membrane association prevent sampling and lead to accumulation of CSP on cellular membranes such as the ER. The coupling of CSP palmitoylation to Golgi membranes may thus be an important requirement for subsequent sorting.

S-Palmitoylation, the attachment of palmitate groups onto cysteine residues via thioester bonds, regulates the membrane interactions of many proteins (1–4). In addition to functioning as a simple membrane anchor, palmitoylation can also regulate protein sorting and the micro-localization of proteins within membranes (5–9). Despite several attempts to identify palmitoyl transferases over many years, it was only relatively recently that palmitoylating enzymes containing a conserved DHHC-CRD (cysteine-rich domain)[2] were first identified in yeast (10, 11), where they mediate the majority of palmitoylation reactions (12). Subsequent analyses in mammalian cells identified a family of 23 proteins containing this conserved DHHC-CRD, and several of these proteins have since been shown to have palmitoyl transferase activity (13–16). Sequence analyses of DHHC proteins predict that they are polytopic membrane proteins, with the DHHC region present on the cytosolic face of the membrane (17). Indeed, the DHHC domain may form part of the enzyme active site (10, 11, 13–15).

The finding that DHHC proteins are integral membrane proteins implies that substrates must contain additional membrane targeting signals to mediate membrane association prior to palmitoylation. This sets palmitoylation apart from isoprenylation and myristoylation, which occur in the cytosol, and indeed these hydrophobic modifications often facilitate membrane association of proteins prior to palmitoylation (*e.g.* H-/N-Ras and Src family kinases). The primary membrane-targeting information contained within many palmitoylated proteins is easily identifiable (myristoyl and isoprenyl attachment sites or transmembrane domains). However, the mechanisms employed by other palmitoylated proteins for initial membrane targeting are less well understood.

Cysteine-string protein (CSP) is a secretory vesicle protein that has been proposed to function in regulated exocytosis pathways in a range of non-neuronal cells and is also essential in the nervous system where it has an important neuroprotective function (18–22). CSP is extensively palmitoylated on up to 14 cysteine residues present within a central CRD (23). CSP lacks transmembrane sequences or isoprenyl/myristoyl consensus sequences, and we recently reported that the CRD of CSP "doubles up" as both a membrane-targeting sequence and a palmitoylation domain (24). Indeed, the minimal membrane-targeting sequence of CSP (amino acids 106–136; cysteine-string domain is 113–136) binds tightly to cell membranes in the

* This work was funded by a Wellcome Trust Research Career Development fellowship (to L. H. C.), by an Medical Research Council Senior Research fellowship (to L. H. C.), and by Tenovus Scotland (Grant S06/1 to L. H. C.). The costs of publication of this article were defrayed in part by the payment of page charges. This article must therefore be hereby marked "*advertisement*" in accordance with 18 U.S.C. Section 1734 solely to indicate this fact.

[S] The on-line version of this article (available at http://www.jbc.org) contains supplemental Figs. S1 and S2.

[1] To whom correspondence should be addressed: Tel.: 44-131-650-8313; Fax: 44-131-650-8313; E-mail: Luke.Chamberlain@ed.ac.uk.

[2] The abbreviations used are: CRD, cysteine-rich domain; DHHC, aspartic acid, histidine, histidine, cysteine; CSP, cysteine-string protein; SNAP25, synaptosomal-associated protein of 25 kDa; GFP, green fluorescent protein; EGFP, enhanced green fluorescent protein; HA, hemagglutinin; BFA, brefeldin A; ER, endoplasmic reticulum.

absence of detectable palmitoylation (24). The identification of residues 106–136 as the minimal membrane-targeting sequence of CSP agrees well with *in silico* analysis suggesting that residues 108–130 have a propensity to move from the aqueous environment to the membrane interface without traversing the bilayer (25). Although membrane-bound, the unpalmitoylated CSP-(106–136) and CSP-(1–136) truncation mutants are mis-sorted in PC12 cells and show extensive overlap with ER markers, suggesting that palmitoylation is essential for correct intracellular sorting of CSP (24).

Two recent elegant studies reported a loss of CSP palmitoylation in the nervous system of DHHC17 mutant *Drosophila*, resulting in defects in presynaptic neurotransmission (26, 27). However, the enzymes that palmitoylate mammalian CSP have not been identified, and indeed it is formally possible that the effects of DHHC17 mutation in *Drosophila* on CSP palmitoylation are indirect. In addition, CSP has a widespread tissue distribution outside the nervous system of both mammals and *Drosophila* (28–30), and it is not clear whether the same DHHC protein(s) palmitoylate CSP in every cell type. To shed light on the pathway of CSP palmitoylation in mammalian cells, we have undertaken a detailed analysis of the DHHC proteins that palmitoylate CSP, identifying a subset of Golgi enzymes that fulfill this function. Furthermore, we present data on the mechanisms that govern intracellular interactions of CSP with its partner DHHC proteins.

EXPERIMENTAL PROCEDURES

Plasmid Constructs, Antibodies, and Chemicals—Mouse DHHC1-DHHC23 clones in pEF-BOS-HA were as previously described (14). Plasmids containing bovine CSP1 fused to an N-terminal GFP tag (pEGFP-C2), CSP4CL and CSP136, CSP137, CSP138, CSP139, and CSP140 truncation mutants were as previously described (20, 24). Note that, as in our previous work (24), the initiating methionine was removed from CSP in all N-terminally tagged constructs. EGFP-SNAP25B was constructed by inserting rat SNAP25B (lacking the initiating N-terminal methionine) into pEGFP-C2. Site-directed mutagenesis was employed to introduce the DHHC-to-DHHS mutations into DHHC3 and DHHC7; the fidelity of all mutant constructs was confirmed by DNA sequencing.

Anti-GFP monoclonal antibody (JL8) was purchased from Clontech. Anti-HA monoclonal antibody and rhodamine-conjugated anti-HA were from Roche Applied Science. Anti-giantin Alexa Fluor 488-conjugated antibody was supplied by Cambridge Bioscience (Cambridge, UK). Rabbit anti-calreticulin polyclonal antibody was from Abcam (Cambridge, UK). Anti-ERGIC53 antibody was from Sigma. Anti-HA Alexa Fluor 488-conjugated monoclonal antibody and all fluorescent secondary antibodies were purchased from Invitrogen.

Proteoextract S-PEK subcellular fractionation kit was purchased from Merck (Nottingham, UK). Lipofectamine 2000 was from Invitrogen. Anti-GFP magnetic isolation kits were obtained from Miltenyi Biotech (Surrey, UK). Promix L-[^{35}S]cysteine/methionine cell labeling mix and Amplify reagent were from Amersham Biosciences. [^{3}H]Palmitic acid was purchased from PerkinElmer Life Sciences. Brefeldin A, nocodazole, and cycloheximide were from Sigma.

Cell Culture and Cell Transfection—PC12 cells were grown in RPMI 1640 medium with 10% horse serum, 5% fetal calf serum, and penicillin/streptomycin. HEK293 cells were cultured in Dulbecco's modified Eagle's medium with 10% fetal calf serum and penicillin/streptomycin. All reagents used for maintenance of cells were purchased from Invitrogen. Cells were maintained in a humidified atmosphere containing 5% CO_2.

For all experiments, cells were plated onto 6-well or 24-well plates that had been precoated with poly-D-lysine. Cells were transfected using Lipofectamine 2000 (Invitrogen) according to the manufacturer's instructions; the ratio of Lipofectamine: DNA used was 2:1.

Effect of DHHC Co-expression on Membrane Association and Palmitoylation of CSP in HEK293 Cells—HEK293 cells on 24-well plates were transfected with EGFP-CSP (0.8 μg) in the presence of individual HA-DHHC clones, empty pEFBOS-HA vector, or mutant DHHCs in which the conserved DHHC motif was mutated to DHHS (1.6 μg). For the dose-dependence analysis of EGFP-CSP palmitoylation by DHHC3 (Fig. 1*C*), 0.8 μg of EGFP-CSP was transfected together with a total of 1.6 μg of empty pEFBOS-HA and HA-DHHC3. The cells were either lysed directly in 200 μl of SDS-dissociation buffer or fractionated into cytosol and membrane fractions (150 μl of each) using an SPEK subcellular proteome extract kit, ~20 h post-transfection. We have previously validated the use of the SPEK kit for separation of cytosolic and membrane proteins (24). Equal volumes of the recovered cytosol and membrane fractions were mixed with SDS-dissociation buffer. All samples were heated to 100 °C for 2 min, separated by SDS-PAGE, and examined by immunoblotting using anti-GFP monoclonal antibody (JL8) or anti-HA. In some experiments, an insoluble (I) fraction was also collected following isolation of cytosol and membrane fractions. For this, cell material remaining after isolation of cytosol and membrane fractions was solubilized in an equivalent volume of SDS-dissociation buffer. Cytosol and membrane bands were quantified (ImageJ) for each sample and expressed as a percentage of membrane association.

For analysis of BFA effects on CSP membrane binding/palmitoylation in HEK293 cells, the cells were incubated for 4 h in transfection mix, which was then removed and replaced with fresh media with or without 30 μg/ml BFA. After a further 4 h, the cells were washed and fractionated into cytosol and membrane fractions and processed as described above.

Analysis of CSP Palmitoylation following BFA Treatment of PC12 Cells—PC12 cells on 24-well plates were transfected with 1 μg of EGFP-CSP, CSP136, or CSP4CL plasmids and used ~40 h post-transfection. For analysis of BFA effects, 30 μg/ml BFA was added directly to the cells and incubated for 1 or 4 h. For some samples, 10 μg/ml cycloheximide was present for 4 h to block new protein synthesis (*e.g.* for the 1-h BFA treatment, cycloheximide was added 3 h before BFA addition). To examine the requirement for intact microtubules, cells were also treated with 10 μg/ml nocodazole for 4 or 6 h. Following treatment, cells were washed, fractionated, and examined by immunoblotting.

Metabolic Labeling—PC12 cells were transfected with 1 μg of DNA and used ~40 h post-transfection. The cells were

washed in Dulbecco's modified Eagle's medium (minus cysteine/methionine) and incubated in the same media for 15 min at 37 °C in the presence of 4–11 MBq/ml [^{35}S]cysteine/methionine Promix. The cells were then washed and incubated at 37 °C for a set time as indicated in the individual figures. Labeled cells were immediately placed on ice and cytosol and membrane fractions isolated using an S-PEK cell fractionation kit (Merck). The entire volume of the isolated fractions was incubated with 15 μl of anti-GFP magnetic beads for 30 min on ice and then added to columns attached to a magnetic plate. The isolated beads were washed four times in lysis buffer and bound proteins eluted by adding 50 μl of SDS-sample buffer preheated to 95 °C. Samples were resolved by SDS-PAGE, and duplicate gels were transferred to nitrocellulose for immunoblotting analysis, or soaked in Amplify reagent (Amersham Biosciences) for 30 min, dried, and examined by autoradiography. For BFA experiments, cells were incubated in 30 μg/ml BFA for 15 min prior to addition of radiolabel, and BFA was also present at the same concentration throughout the pulse-chase period. [^{3}H]Palmitate labeling experiments were performed as previously described (24). Band intensities were calculated using ImageJ and used to calculate percent membrane association and palmitoylation.

Antibody Staining of Fixed Cells and Confocal Imaging—Transfected HEK293 cells were washed in phosphate-buffered saline and fixed in 4% formaldehyde for 30 min at room temperature. In some experiments, cells were incubated in 30 μg/ml BFA and 10 μg/ml cycloheximide for 90 min prior to fixation. The fixed cells were then permeabilized for 10 min in phosphate-buffered saline/0.25% Triton X-100. Cells were then labeled for 1 h with a range of primary and secondary antibodies (in phosphate-buffered saline/0.3% bovine serum albumin) at the following dilutions: rhodamine- or fluorescein isothiocyanate-conjugated anti-HA, 1:100; anti-ERGIC53 and anti-calreticulin, 1:50; anti-giantin Alexa Fluor 488, 1:200; Alexa Fluor labeled secondary antibodies, 1:200. The cells were then washed, and the coverslips were mounted onto glass slides in Mowiol. PC12 cells transfected with EGFP-CSP4CL or DHHC17-EGFP were fixed in 4% formaldehyde following BFA treatments and washout and mounted in Mowiol. Imaging was performed on a Zeiss LSM510 confocal laser scanning microscope. Image data acquired at Nyquist sampling rates were deconvolved using Huygens software (Scientific Volume Imaging).

PCR Analysis—To examine DHHC mRNA expression, total RNA was purified from PC12 cells using an RNeasy kit (Qiagen). Reverse transcription was performed using ImProm-II reverse transcriptase (Promega). PCR amplifications were set up using either 20 ng of DHHC plasmid DNA or 5 μl from a 20-μl reverse transcription reaction. Primers used were designed based on the sequence of rat DHHCs and were as follows: DHHC3 forward, CTTATGATGCTTATCCCCACTCATCAC; DHHC3 reverse, TCAGACCACATACTGGTACGGGTC; DHHC7 forward, CATGCAGCCGTCAGGACACAGGCTCC; DHHC7 reverse, TCATACAGAGAACTCGGGGCCTC; DHHC15 forward, GAAGAGAGACCTGAGGTCCAGAAGCAG; DHHC15 reverse, CTATGTTTCTGACTCCACAGCAAGTG; DHHC17 forward, GAAGCTGGAGGGAACGTGGATGCCC; and DHHC17 reverse, CTACACCAGCTGGTACCCAGATCC. Primers (10 pmol) and GoTaq PCR master mix (Promega, Madison, WI) were added to the DNA templates. PCR consisted of 30 cycles of 94 °C for 30 s, 58 °C for 30 s, and 72 °C for 90 s.

Statistical Analysis—All averaged data are expressed as means ± S.E. Data were analyzed using unpaired Student's *t* test.

RESULTS AND DISCUSSION

CSP Palmitoylation Is Inefficient in HEK293 Cells and Is Enhanced by Co-expression of Specific Golgi-localized DHHC Proteins—As previously shown (24), when EGFP-CSP is expressed in PC12 cells, two bands are specifically detected by immunoblotting (Fig. 1*A*). The lower molecular weight band (indicated by an *arrowhead*) represents unpalmitoylated CSP and does not incorporate [^{3}H]palmitate, whereas the upper band is fully palmitoylated and strongly incorporates radiolabel (Fig. 1*A*) (24). This change in migration that occurs following the extensive palmitoylation of CSP is well documented (23–25, 31–34). Indeed, the upper band migrates at the same size as the lower band following chemical depalmitoylation of CSP (see for example Ref. 24). Employing this band-shift to measure CSP palmitoylation is a very useful approach, not least because it provides an accurate and quantitative assessment of the proportion of CSP molecules that are palmitoylated. In addition, as partially palmitoylated CSP molecules can be distinguished from fully palmitoylated protein by migration on polyacrylamide gels (24), this analysis provides data on the extent of palmitoylation of individual molecules. Similar approaches employing [^{3}H]palmitate labeling do not allow a direct analysis of either the proportion of molecules that are palmitoylated or the level of palmitoylation of individual molecules.

Whereas the upper palmitoylated band is the major form of EGFP-CSP in transfected PC12 cells, only a small pool of the protein is palmitoylated when expressed in HEK293 cells (Fig. 1*A*). This suggests that only a limited amount of palmitoyl transferases active against CSP are expressed in HEK293 cells, and thus, we employed this cell type to characterize the palmitoylation of CSP in mammalian cells. Recent work identified a family of 23 putative mammalian palmitoylating enzymes containing a conserved DHHC motif (14). Although several of these DHHC proteins have been shown to have palmitoyl transferase activity, at present a complete screen of all DHHC proteins for such activity is lacking. We co-transfected HEK293 cells with EGFP-CSP and HA-tagged versions of each of the 23 DHHC proteins. Interestingly, CSP palmitoylation was markedly enhanced by DHHC3, DHHC7, DHHC15, and DHHC17 (Fig. 1*B*). To ensure that the observed enhancement of CSP palmitoylation was directly related to DHHC protein expression, we examined the effects of increasing amounts of DHHC3 plasmid (while maintaining the total amount of transfected DNA) on palmitoylation of co-transfected EGFP-CSP. Fig. 1*C* clearly shows that increased palmitoylation of CSP was directly related to expression levels of DHHC3.

Note that some of the DHHC proteins were poorly expressed in HEK293 cells (Fig. 1*D*), and thus the identification of four enzymes that palmitoylate CSP may be an underestimate. However, many non-active DHHC proteins were expressed at sim-

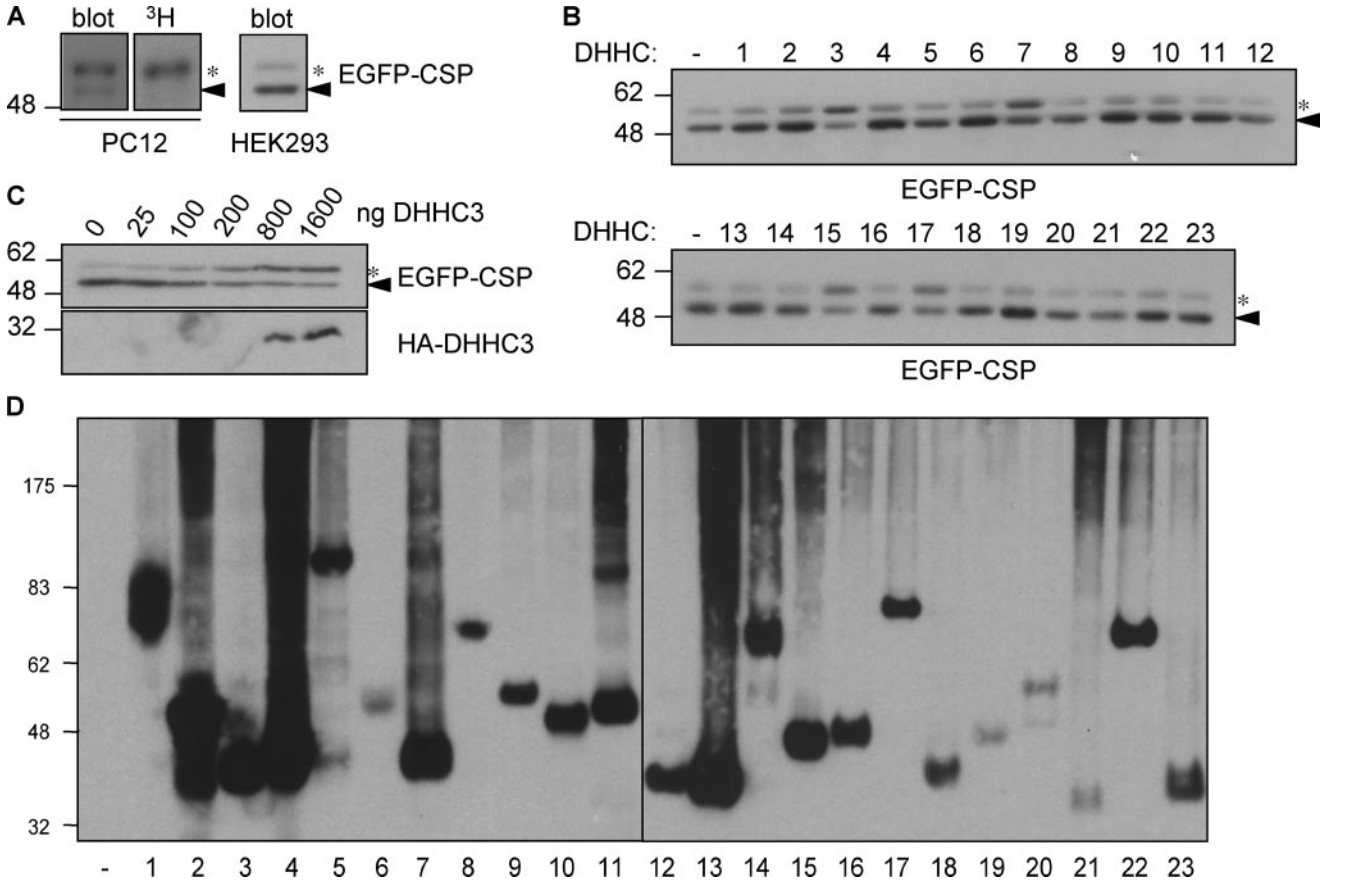

FIGURE 1. **DHHC proteins mediate CSP palmitoylation.** *A*, *left panel*, PC12 cells transfected with EGFP-CSP were incubated in [^{3}H]palmitate for 4 h. Cells were lysed and EGFP-CSP recovered by immunoprecipitation. Precipitated samples were resolved by SDS-PAGE and transferred to nitrocellulose for immunoblotting analysis using monoclonal anti-GFP (*blot*) or processed for fluorographic detection of incorporated radiolabel (*^{3}H*). *Right panel*, a lysate from HEK293 cells transfected with EGFP-CSP probed by immunoblotting with anti-GFP. *B*, HEK293 cells were transfected with EGFP-CSP together with empty pEFBOS-HA (−) or with each of the 23 DHHC constructs (numbered 1–23). Lysates were prepared from transfected cells ~20 h post-transfection and resolved by SDS-PAGE and transferred to nitrocellulose for immunoblotting analysis using anti-GFP. *C*, EGFP-CSP plasmid together with the indicated amounts of DHHC3 vector were transfected into HEK293 cells. Note that the total amount of plasmid in each sample was maintained constant by including empty pEFBOS-HA vector in appropriate amounts. Lysates were prepared from the transfected cells, resolved by SDS-PAGE, and transferred to nitrocellulose for immunoblotting analysis using anti-GFP or anti-HA. *D*, lysates were prepared from HEK293 cells transfected with each of the 23 DHHC proteins and probed by immunoblotting with anti-HA. The position of molecular weight standards is shown on the left side of all panels; *asterisks* denote palmitoylated CSP and *arrowheads* indicate unpalmitoylated CSP.

ilar or higher levels than DHHC3/7/15/17, confirming the specificity of the results. The identification of DHHC17 as an enzyme that palmitoylates mammalian CSP agrees well with recent analyses of *Drosophila* mutants (26, 27). Previous work has reported co-localization of DHHC3/7/15/17 with Golgi markers (13, 15, 35), and we confirmed co-localization of these proteins with the cis/medial Golgi protein giantin in HEK-293 cells (Fig. 2).

We also compared the distribution of the DHHC proteins with the ER-Golgi intermediate compartment protein ERGIC-53 (supplemental Fig. S1). The ERGIC-53 signal was present in puncta throughout the cytosol with some enrichment in a region of the cell that was closely positioned, although clearly distinct from the DHHC proteins. Thus, DHHCs 3, 7, 15, and 17 are mainly localized to the Golgi with only minimal overlap with the ER-Golgi intermediate compartment.

Several other DHHC proteins are also localized to the Golgi in HEK293 cells (data not shown and see reference (35)), and hence there is clearly substrate specificity within this Golgi subset of DHHC proteins. It will be interesting to determine the factors that regulate this substrate specificity.

DHHC Proteins Regulate Stable Membrane Binding of CSP—In PC12 cells, palmitoylated EGFP-CSP associates tightly with membranes (Fig. 3*A*) (24). We recently proposed that the hydrophobic cysteine-string domain of CSP facilitates membrane anchoring prior to palmitoylation (24). However, it is not clear whether this interaction is stable or weak/transient. The inefficient palmitoylation of EGFP-CSP in HEK293 cells allowed us to address this question. Indeed, despite the large fraction of unpalmitoylated EGFP-CSP in HEK293 cells, we did not detect any significant quantity of this unpalmitoylated protein in the membrane fraction (Fig. 3*A*). This suggests that the CRD is not able to mediate stable membrane binding of full-length CSP in the absence of palmitoylation. Confocal imaging also revealed a dispersed, mainly cytosolic localization of EGFP-CSP in HEK293 cells (Fig. 3*B*). Because specific DHHC proteins enhance CSP palmitoylation in HEK293 cells (Fig. 1*B*), we therefore tested whether these enzymes were sufficient to catalyze stable membrane binding of CSP. Thus, HEK293 cells were co-transfected with EGFP-CSP and each of the 23 HA-tagged DHHC constructs and subsequently fractionated into cytosol and membrane fractions. As with the analyses of whole

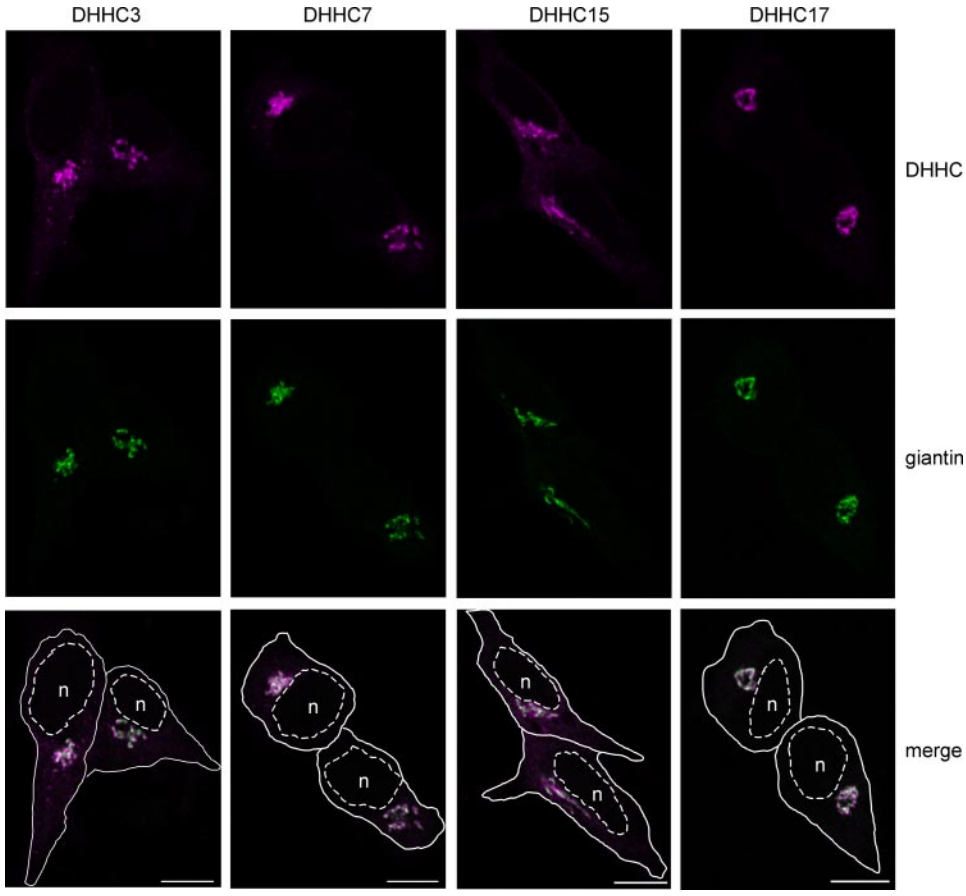

FIGURE 2. **Analysis of HA-DHHCs and giantin localization in HEK293 cells.** HEK cells plated on coverslips were transfected with HA-tagged DHHC constructs and ~20 h later were fixed, permeabilized, and stained with Alexa Fluor 488-conjuagted anti-giantin (1:200) and rhodamine-conjugated anti-HA (1:100). The coverslips were then mounted in Mowiol and imaged using a Zeiss LSM510 Axiovert laser scanning confocal microscope. For clarity, a rough outline of the cell membranes (*solid line*) and the nuclei (*dashed line*, *n*) is shown for the *merged images*. *Scale bars* represent 10 μm.

cell lysates, DHHC3, DHHC7, DHHC15, and DHHC17 specifically and significantly enhanced palmitoylation of EGFP-CSP, and the palmitoylated protein was exclusively present in the membrane fraction (Fig. 3, *C* and *D*). Thus, expression of these specific DHHC proteins is sufficient to catalyze the extensive palmitoylation of CSP and to promote its stable membrane attachment. Interestingly, DHHC11 coexpression consistently reduced CSP membrane interaction. To ensure that the effects observed upon co-expression of specific DHHC proteins were directly related to the enzymatic activity of the proteins, we introduced inactivating point mutations into the DHHC domains of both DHHC3 and DHHC7 as previously described (10, 11, 13–15). Despite being expressed at similar levels as the wild-type DHHC3/7 proteins, these inactive mutants had no stimulatory effect on CSP palmitoylation/membrane binding in HEK293 cells, and indeed both mutants inhibited CSP palmitoylation (significant only for DHHC3) (Fig. 3*E*). As a further control, we confirmed that the prepared cytosol and membrane fractions contained the entire pool of transfected EGFP-CSP with no protein remaining in the insoluble cell fraction (Fig. 3*F*).

We next examined whether the DHHC enzymes that palmitoylate CSP in transfected HEK293 cells are expressed in PC12 cells. For this, RT-PCR was performed on RNA purified from PC12 cells. Fig. 3*G* shows that amplification products of the expected size were obtained from PCR reactions using DHHC3, DHHC7, or DHHC17 primers. In contrast we did not detect a signal for DHHC15 by RT-PCR (Fig. 3*G*). However, when an aliquot of the DHHC15 RT-PCR was subjected to a second round of PCR a faint band was now visible (data not shown). The results of the PCR amplifications were obtained using two independent RNA samples.

Correlation between Enhanced Membrane Affinity of CSP Mutants, Palmitoylation, and Intracellular Localization—We previously identified two unpalmitoylated CSP mutants that were localized predominantly to the ER in PC12 cells; these mutants either contained a truncation of the C terminus immediately after the cysteine-string domain (CSP136) or replacement of 4 cysteines in the cysteine-string domain with leucine residues (CSP4CL) (24). Based upon the results of current experiments showing localization of CSP-palmitoylating DHHC proteins to Golgi membranes, we reasoned that the lack of palmitoylation of CSP136 and CSP4CL might be related to perturbations of initial membrane interactions, leading to accumulation of these mutants on 'inappropriate' membranes. It is not easy to determine if CSP136 and CSP4CL have an altered membrane affinity relative to wild-type CSP in PC12 cells due to efficient palmitoylation of the wild-type protein in this cell type (24). Thus, we analyzed membrane binding in HEK293 cells, which express only limited amounts of DHHC protein(s) active against CSP. This analysis clearly revealed that both CSP136 and CSP4CL associated more tightly with membranes than wild-type CSP (Fig. 4*A*). Comparing the intracellular localizations of the two mutants with HA-DHHC3 in HEK293 cells highlighted a clear physical separation of the CSP mutants from the Golgi-localized DHHC protein (Fig. 4*B*); as in PC12 cells, both CSP mutants exhibited an ER-like distribution, similar to the ER resident protein calreticulin (Fig. 4*B*, *bottom panel*). Thus, CSP mutants that enhance membrane affinity promote association with "inappropriate" cell membranes, offering one explanation for the finding that these mutants are not efficiently palmitoylated in PC12 cells (24). In support of this idea, neither CSP136 nor CSP4CL were palmitoylated when co-transfected with DHHC3 or DHHC7 in HEK293 cells (see Fig. 8*A*).

Interestingly, the level of membrane binding of CSP truncation mutants expressed in HEK293 cells decreased significantly as amino acids were added to the C terminus of the cysteine-

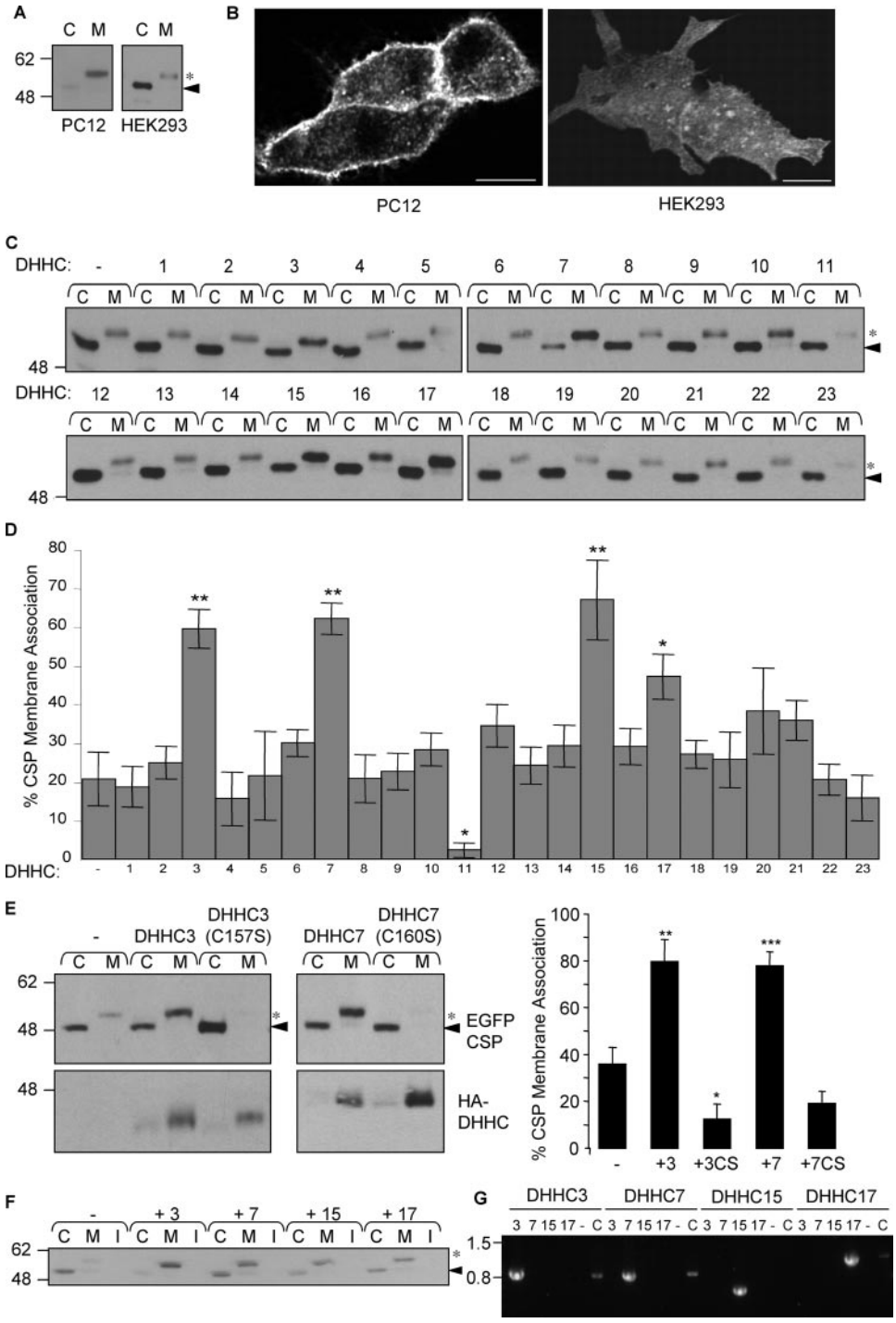

FIGURE 3. **DHHC proteins regulate CSP membrane binding.** *A*, PC12 and HEK293 cells were transfected with EGFP-CSP and fractionated into cytosol (*C*) and membrane (*M*) fractions. Equal volumes of the recovered samples were resolved by SDS-PAGE and transferred to nitrocellulose for immunoblotting analysis using anti-GFP. *B*, confocal images of EGFP-CSP distribution in PC12 cells and HEK293 cells. *Scale bars* represent 10 μm. *C*, HEK293 cells were transfected with EGFP-CSP in the absence (−) or presence of each of the 23 HA-tagged DHHC constructs. The cells were processed as described for *A*. *D*, the percent membrane association ± S.E. of EGFP-CSP transfected together with each of the DHHC proteins (indicated by 1–23) was determined by densitometry, and the averaged data are presented ($n = 5$). *, p value of <0.03; **, p value of <0.004 compared with CSP in the absence of DHHC co-expression. *E*, HEK293 cells were co-transfected with EGFP-CSP and wild-type HA-tagged DHHC3/DHHC7 or with the inactive DHHC mutants, DHHC3 (C157S)/DHHC7 (C160S). Cells were fractionated into cytosol (*C*) and membrane (*M*) fractions, and equal volumes were resolved by SDS-PAGE, transferred to nitrocellulose, and probed with antibodies against GFP and HA. Representative blots are shown in the *left panel*. The *right panel* shows the percent membrane association ± S.E. of EGFP-CSP under the different transfection conditions determined by quantification of immunoblots ($n = 6$). *, p value of <0.03, **, p value of <0.003, and ***, p value of <0.0006 compared with EGFP-CSP in the absence of DHHC expression. *F*, HEK293 cells were co-transfected with EGFP-CSP and DHHC3, DHHC7, DHHC15, or DHHC17 and fractionated into cytosol (*C*) and membrane (*M*) fractions. The remaining insoluble (*I*) cell material was solubilized in SDS-dissociation buffer. Equal volumes of the recovered fractions were resolved by SDS-PAGE and transferred to nitrocellulose for immunoblotting analysis using anti-GFP. *G*, primers recognizing DHHC3, DHHC7, DHHC15, and DHHC17 were used in PCR reactions that contained purified plasmid DNA (*3*, DHHC3 template; *7*, DHHC7 template; *15*, DHHC15 template; *17*, DHHC17 template), no DNA (−) or cDNA (*C*). Position of selected standards (in kilobase pairs) is shown on the *left*. The predicted sizes of amplification products were: DHHC3, 903 bp; DHHC7, 928 bp; DHHC15, 716 bp; and DHHC17, 1164 bp. The position of molecular weight standards is shown on the *left side* of all *panels*; *asterisks* denote palmitoylated CSP, and *arrowheads* indicate unpalmitoylated CSP.

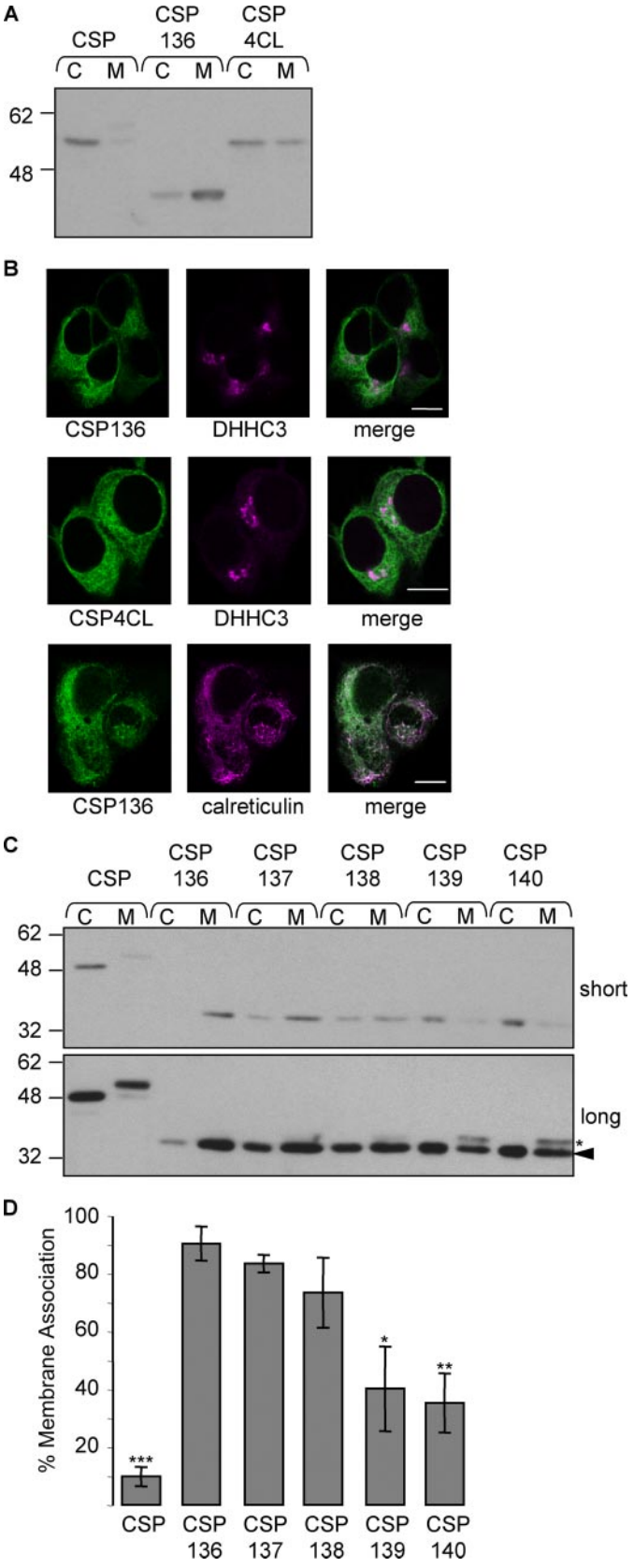

FIGURE 4. **Membrane binding and palmitoylation of CSP mutants.** *A*, HEK293 cells transfected with EGFP-CSP, CSP136, or CSP4CL were fractionated into cytosol (*C*) and membrane (*M*) fractions ~20 h post-transfection. Equal volumes of the recovered fractions were resolved by SDS-PAGE and analyzed by immunoblotting using anti-GFP. *B*, HEK293 cells were transfected with EGFP-CSP136 and HA-DHHC3 (*top panel*), EGFP-CSP4CL and HA-DHHC3 (*middle panel*), or with EGFP-CSP136 alone (*bottom panel*). Cells were fixed, permeabilized, and incubated with rhodamine-conjugated anti-HA (1:100) (*top* and *middle panels*) or with anti-calreticulin antibody (1:50) followed by Alexa Fluor 543-conjugated rabbit secondary antibody (1:200, *bottom panel*). Coverslips were mounted in Mowiol and examined using a Zeiss LSM510 Axiovert laser scanning confocal microscope. *Scale bars* represent 10 μm. *C*, HEK293 cells were transfected with wild-type EGFP-CSP and the indicated C-terminal truncation mutants. Cells were then fractionated into cytosol (*C*) and membrane (*M*) fractions, which were examined by immunoblotting with anti-GFP. Shown is a short and long exposure of the same blot. *D*, averaged data ± S.E. for percent membrane binding of the mutants analyzed in *panel C* ($n = 5$). *, p value of <0.02; **, p value of <0.002; and ***, p value of <0.000008 compared with CSP136. For all immunoblots shown, the positions of molecular weight standards are shown on the *left*; *arrowheads* indicate unpalmitoylated CSP, whereas *asterisks* highlight palmitoylated CSP.

string domain, and the presence of Lys^{137}-Pro^{138}-Lys^{139} in the CSP139 mutant weakened membrane binding significantly (Fig. 4, *C* and *D*). Strikingly, this loss of membrane binding correlated near perfectly with the appearance of a palmitoylated fraction of EGFP-CSP (Fig. 4*C*, *asterisk*) (24), further highlighting the inverse correlation between membrane affinity of CSP mutants and palmitoylation.

Membrane Binding and Palmitoylation of CSP Are Insensitive to BFA—The results presented thus far are consistent with the notion that wild-type CSP likely has a weak membrane affinity (mediated by the cysteine-string domain), which is enhanced either by C-terminal truncation or by the introduction of more hydrophobic amino acids. To determine whether wild-type CSP has a specific affinity for Golgi membranes or a more general membrane affinity, we examined the effects of BFA on membrane binding and palmitoylation. BFA inhibits the function of ARF1 (36, 37), a protein essential for vesicle budding from the ER. BFA treatment thus blocks ER-to-Golgi transport and promotes a loss of Golgi integrity and fusion of Golgi membranes with the ER (37). In a first set of experiments, HEK293 cells were transfected with EGFP-CSP with or without DHHC3 or DHHC7. 4 h post-transfection, the cells were incubated in the presence or absence of 30 μg/ml BFA for a further 4 h and subsequently fractionated. In this experimental set-up, BFA will prevent the trafficking of co-transfected DHHC3 and DHHC7 from the ER. Fig. 5 (*A* and *B*) shows that BFA treatment did not inhibit membrane binding or palmitoylation of EGFP-CSP either in the absence or presence of DHHC co-transfection. This result implies that CSP palmitoylation does not require a specific intracellular localization of partner DHHC proteins, but only sufficient cellular expression levels. These results are thus consistent with the notion that CSP has a general membrane affinity rather than recognizing specific features inherent to intact Golgi membranes.

Because BFA had no effect on membrane binding or palmitoylation of EGFP-CSP, we checked whether this drug was having the expected effects on Golgi proteins. BFA was thus added to cells transfected with HA-DHHC3; this treatment clearly promoted the redistribution of HA-DHHC3 from a tight ribbon-like morphology to a dispersed localization (Fig. 5*C*). Staining was visible around the nucleus, consistent with at least partial redistribution to the ER. The presence of cycloheximide in these experiments ensures that the observed localization of DHHC3 represents a redistribution of the protein rather than

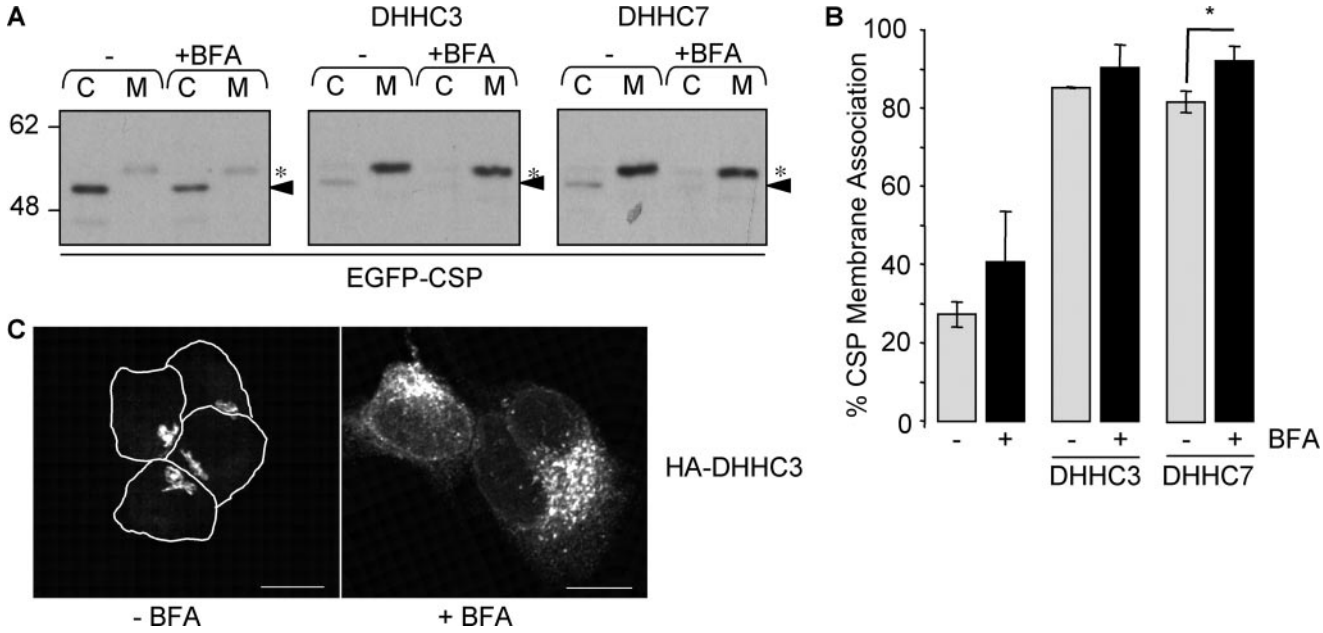

FIGURE 5. **Effect of BFA on CSP palmitoylation and membrane association in HEK293 cells.** *A*, HEK293 cells were transfected with EGFP-CSP in the presence/absence of DHHC3 or DHHC7. 4 h after transfection, fresh medium was added either with or without 30 μg/ml BFA and, after an additional 4 h, the cells were fractionated into cytosol (*C*) and membrane (*M*) fractions. Equal volumes of the fractions were probed with an antibody against GFP. Positions of molecular weight standards are shown on the *left*. *Arrowheads* indicate unpalmitoylated CSP, whereas *asterisks* highlight palmitoylated CSP. *B*, averaged data ± S.E. for percent membrane binding of EGFP-CSP in the absence or presence of DHHC3/7 co-expression and with or without BFA treatment ($n = 3$). *, p value of <0.05. *C*, cells were transfected with HA-DHHC3 and ~20 h later were incubated in the absence (*left panel*) or presence (*right panel*) of 30 μg/ml BFA/10 μg/ml cycloheximide for 90 min. The cells were then washed, fixed, permeabilized, stained with Alexa Fluor 488-conjugated anti-HA, and examined using a Zeiss LSM510 Axiovert laser scanning confocal microscope. For clarity, a rough outline of the cell membranes (*solid line*) is shown for untreated cells (*-BFA*). *Scale bars* represent 10 μm.

trapping of newly synthesized protein. Thus, BFA has the expected effects on Golgi-localized DHHC proteins in HEK293 cells.

To extend these observations and to determine whether CSP membrane association and palmitoylation is also BFA-resistant in a cell type that expresses endogenous CSP, we examined membrane binding/palmitoylation of EGFP-CSP in PC12 cells. Due to lower transfection efficiencies in this cell type, we were unable to detect protein expression by immunoblotting 8 h post-transfection. Thus, we performed [^{35}S]cysteine/methionine pulse-chase experiments to follow membrane binding and palmitoylation specifically of newly synthesized EGFP-CSP. As a first step we examined the time course of membrane association and palmitoylation by labeling the cells for 15 min and then removing the radiolabel and fractionating the cells after an additional 15–60 min (Fig. 6*A*). Two significant observations were made from this experiment: (i) there was a time-dependent appearance of palmitoylated CSP on membranes (*asterisk*); (ii) although unpalmitoylated CSP (*arrowhead*) was clearly associated with membranes, the level of membrane association of unpalmitoylated CSP was relatively constant over time. This would be expected if a protein with a weak membrane affinity was transiently associating to cell membranes.

Having established that CSP palmitoylation was readily detectable following a 60-min "chase" period, we next examined the effects of BFA treatment on membrane binding and palmitoylation of newly synthesized EGFP-CSP in PC12 cells. Thus, ~40 h post-transfection, cells were incubated with or without BFA for 15 min. The cells were then incubated in radiolabel for 15 min, washed and incubated for a further 60 min in the presence/absence of BFA. CSP palmitoylation in this assay is dependent upon endogenous DHHC proteins; BFA treatment will promote redistribution of Golgi DHHC proteins to a fused ER-Golgi compartment. As a control, we examined the effects of BFA treatment in this assay on the membrane association of EGFP-SNAP25; as previously described (38) the membrane attachment of this palmitoylated protein was significantly inhibited by BFA treatment (Fig. 6*B*). In contrast, BFA had no significant effect on either palmitoylation or membrane association of radiolabeled EGFP-CSP (Fig. 6, *C* and *D*). Thus, in both HEK293 cells and PC12 cells, membrane binding and palmitoylation of EGFP-CSP is independent of Golgi integrity or intracellular distribution of DHHC proteins. These results support the notion that CSP has a general (and weak) membrane affinity and that stable membrane attachment requires only sufficient cellular expression of appropriate DHHC proteins.

Brefeldin A Treatment Promotes Palmitoylation of CSP4CL but Not CSP136—Having found that CSP-palmitoylating DHHC proteins retain activity after BFA treatment, we reasoned that BFA-mediated redistribution of Golgi-localized DHHC proteins to the ER might facilitate palmitoylation of the ER-localized CSP mutants. These experiments would thus allow us to determine whether CSP4CL and CSP136 are unpalmitoylated because they are present on distinct membranes to their partner DHHC proteins, or alternatively whether structural changes in the mutant proteins prevent their palmitoylation.

Thus, we examined the effects of BFA treatment on palmitoylation of CSP136 and CSP4CL in PC12 cells. We did not

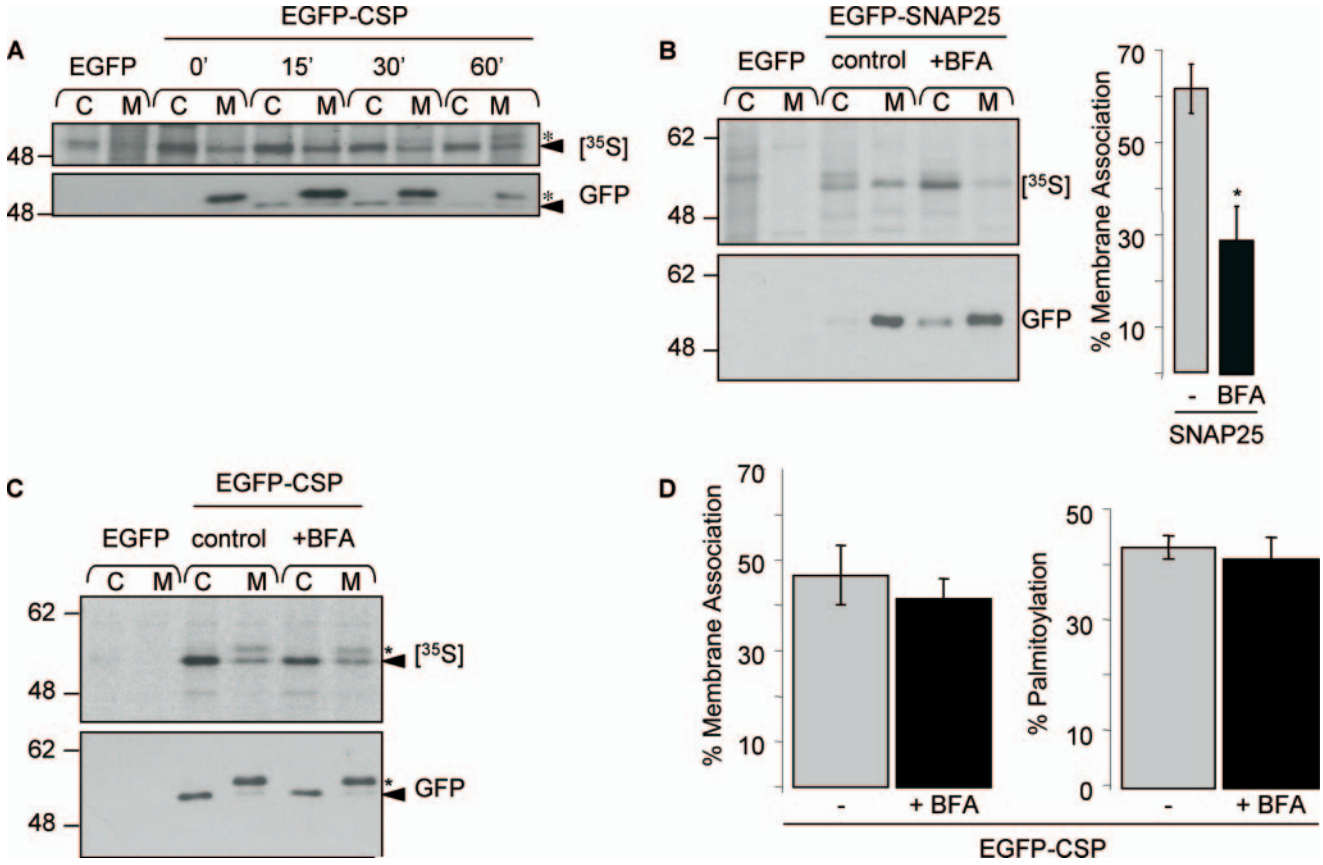

FIGURE 6. **BFA does not affect membrane binding or palmitoylation of EGFP-CSP in PC12 cells.** *A*, PC12 cells transfected with EGFP-CSP or empty vector (EGFP) were incubated with ^{35}S-labeled cysteine/methionine for 15 min, washed, and chased for various times as indicated ranging from 0 to 60 min. The labeled cells were fractionated into cytosol (*C*) and membrane (*M*) fractions, from which GFP-tagged proteins were recovered by immunoprecipitation and subsequently analyzed by immunoblotting with anti-GFP (*GFP*). Duplicate gels were developed using autoradiography (*[^{35}S]*). Note that the ^{35}S-labeled band detected in the EGFP cytosol fraction is a nonspecific band that migrates more slowly than cytosolic EGFP-CSP. *B*, cells were transfected with EGFP-SNAP25B. Approximately 40 h post-transfection, the cells were incubated in the absence or presence of 30 μg/ml BFA for 15 min, and then incubated in ^{35}S-labeled cysteine/methionine for 15 min, washed, and chased for a further 60 min (for BFA samples, BFA was present throughout the pulse-chase period). The labeled cells were fractionated into cytosol (*C*) and membrane (*M*) fractions, from which EGFP-SNAP25B was recovered by immunoprecipitation and subsequently analyzed by immunoblotting with anti-GFP (*GFP*). Duplicate gels were developed using autoradiography (*[^{35}S]*). The percent membrane binding ± S.E. of EGFP-SNAP25 in the presence and absence of BFA was determined by densitometry of autoradiographs. *, *p* value of <0.005 compared with EGFP-SNAP25 in the absence of BFA. *C*, cells transfected with EGFP-CSP were treated as described for SNAP25. *D*, the percent membrane binding ± S.E. of EGFP-CSP in the presence and absence of BFA was determined by densitometry of autoradiographs (*left panel*). The percent palmitoylation of EGFP-CSP was determined as a percentage of the total membrane-bound pool (*right panel*). *Arrowheads* indicate unpalmitoylated CSP, whereas *asterisks* denote palmitoylated CSP. The positions of molecular weight standards are shown on the *left* of all *panels*.

detect any effect of BFA treatment on the palmitoylation status of either wild-type CSP or CSP136 (Fig. 7*A*). Intriguingly though, we observed a robust palmitoylation of CSP4CL after as little as 1 h of BFA treatment (Fig. 7*A*). This observation suggests that BFA-induced mixing of ER and Golgi membranes allows access of Golgi DHHC proteins to CSP4CL, facilitating the palmitoylation of this mutant. The effects of BFA were likely attributable to redistribution of Golgi enzymes to the ER rather than "trapping" of newly synthesized DHHC proteins in the ER, because treatment with cycloheximide to block protein synthesis did not affect BFA-induced palmitoylation of CSP4CL (Fig. 7*B*). As an additional control, we also examined the effects of nocodazole on the BFA-induced palmitoylation of CSP4CL; nocodazole prevents the assembly of microtubules, which are required for BFA-induced fusion of ER and Golgi membranes (39). As can be seen in Fig. 7*C* the presence of nocodazole blocked BFA-induced palmitoylation of CSP4CL, implying that ER-Golgi fusion is essential for the effects observed. Overall, these results in PC12 cells are particularly relevant as they strongly support the conclusion that DHHC proteins active against CSP are localized predominantly to the Golgi. Furthermore, they support the notion that lack of CSP4CL palmitoylation results from a physical separation of this mutant from these Golgi-localized DHHC proteins.

Note that these experiments were performed ~40 h post-transfection and thus following extensive intracellular accumulation of unpalmitoylated CSP4CL, emphasizing the efficiency of BFA-induced palmitoylation; roughly 40% of the intracellular CSP4CL was palmitoylated within 1 h of BFA treatment (Fig. 7). In comparison, only around 20% of wild-type CSP produced during a 15-min labeling period was palmitoylated within a similar time frame (Fig. 6). These results therefore suggest that, following BFA-induced re-localization of Golgi enzymes to the ER, palmitoylation of CSP4CL is more efficient than palmitoylation of wild-type CSP. The most likely explanation for these findings is that, whereas palmitoylation of CSP is limited by its weak membrane affinity, the tighter membrane binding of

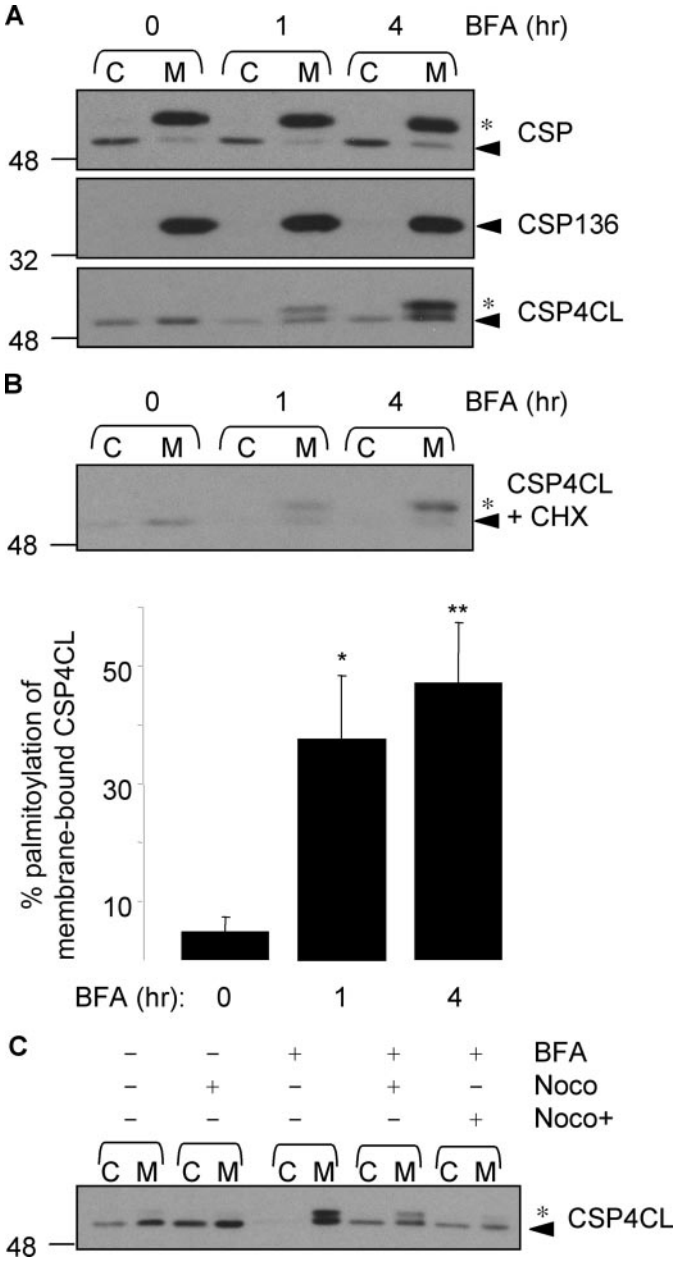

FIGURE 7. **Effect of BFA on palmitoylation of CSP proteins in PC12 cells.** *A*, PC12 cells transfected with EGFP-CSP, CSP136, or CSP4CL were treated with 30 μg/ml BFA for 1 or 4 h or left untreated (*0*). The cells were then fractionated into cytosol (*C*) and membrane (*M*) fractions, and equal volumes of each fraction were separated by SDS-PAGE and transferred to nitrocellulose for immunoblotting analysis using anti-GFP. *B*, as in *panel A* except shown only for EGFP-CSP4CL, which was treated with or without BFA in the presence of 10 μg/ml cycloheximide (*CHX*). The *top panel* shows a representative immunoblot, whereas the *bottom panel* shows averaged data ± S.E. for percent palmitoylation of membrane-bound CSP4CL ($n = 5$). *, p value of <0.02 and **, $p < 0.003$ compared with percent palmitoylation in the absence of BFA treatment. *C*, cells were incubated for 4 h with or without 30 μg/ml BFA in the presence or absence of 10 μg/ml nocodazole as indicated. *Noco+* indicates where nocodazole was added 2 h before the addition of BFA and maintained throughout BFA treatment. Cycloheximide (10 μg/ml) was present in all samples. For all immunoblots shown, the positions of molecular weight standards are shown on the *left*, and unpalmitoylated and palmitoylated CSP bands are indicated by *arrowheads* and *asterisks*, respectively.

CSP4CL ensures a faster rate of palmitoylation when Golgi enzymes are re-localized to the ER.

HEK293 cells contain sufficient DHHC proteins to palmitoylate only a small pool of wild-type CSP (Figs. 1, 3, and 5). We reasoned that, if the extent of CSP palmitoylation is regulated by (i) the transient nature of membrane association of unpalmitoylated CSP and (ii) the expression levels of DHHC proteins, then the enhanced membrane affinity of CSP4CL should facilitate a more efficient palmitoylation of this mutant in BFA-treated HEK293 cells than observed for wild-type CSP. To test this idea, we performed BFA experiments in HEK293 cells transfected with CSP4CL and CSP136 (as described for Fig. 5). As predicted, BFA treatment of HEK293 cells promoted an increase of ~7-fold in the extent of CSP4CL palmitoylation, with ~70% of the protein palmitoylated following BFA treatment (Fig. 8). This was in contrast to the almost complete lack of CSP4CL palmitoylation when transfected either in the absence or presence of DHHC3/7 but without BFA-induced mixing of ER/Golgi membranes (Fig. 8*A*). Thus, when localized to the same intracellular compartment as partner DHHC proteins, the enhanced membrane affinity of CSP4CL facilitates a faster rate of palmitoylation.

As in PC12 cells, CSP136 was not palmitoylated in BFA-treated HEK293 cells, either in the absence or presence of DHHC3/7 co-expression (Fig. 8*A*). The inability of BFA treatment to promote palmitoylation of CSP136 suggests that residues in the C terminus (such as Lys^{137}-Pro^{138}-Lys^{139}) are important for palmitoylation. Indeed, we previously reported that a CSP(K137A) mutant was not efficiently palmitoylated in PC12 cells (24). The CSP136 mutant might also adopt a membrane orientation that indirectly prevents palmitoylation. For example, it is possible that the lack of a significant amount of charged residues at the C-terminal end of CSP136 results in the protein "slipping" into the membrane interior, thus preventing interaction with DHHC proteins.

CSP4CL Does Not Noticeably Redistribute following BFA Washout—Palmitoylation plays an important role in the trafficking of many proteins (3). To determine if CSP palmitoylation is always coupled to forward transport in the secretory pathway, we performed BFA washout experiments (37) to analyze whether palmitoylated CSP4CL protein is able to traffic from the ER. As a control for a Golgi protein, we transfected cells in parallel with EGFP-tagged DHHC-17. Cells were either treated with BFA for 2 h in the presence of cycloheximide, or treated with BFA/cycloheximide, washed five times in fresh media containing cycloheximide but without BFA, and allowed to recover for 4 h. Cells were fixed and examined by confocal imaging. As shown in Fig. 9*A*, DHHC17 showed the expected distributions: Golgi in control cells, dispersed after BFA treatment and Golgi following BFA washout. To quantify these changes we examined DHHC17 distribution and scored the cells for either Golgi localization or dispersed (ER) distribution (Fig. 9*B*).

Interestingly, and in contrast to DHHC17, we did not detect any changes in the distribution of CSP4CL following BFA washout (Fig. 9*A*). This finding suggests that palmitoylation is not sufficient to direct exit of CSP4CL from the ER. We speculate that the amino acid sequence/structure of palmitoylated CSP facilitates the movement into budding vesicle at the Golgi but not at the ER. Thus, the specific intracellular compartment at which CSP is palmitoylated, and hence stably anchored to, is likely to play a major role in determining targeting specificity.

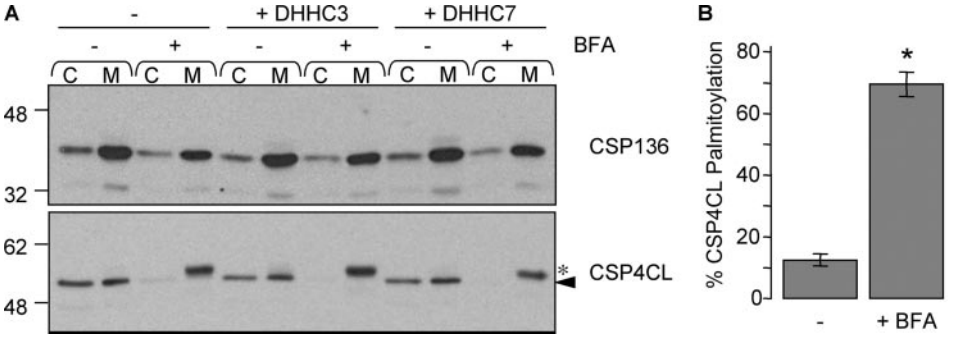

FIGURE 8. **Effect of BFA on palmitoylation of CSP proteins in HEK293 cells.** Cells were transfected with EGFP-CSP136 or EGFP-CSP4CL in the presence or absence of HA-DHHC3/7. 4 h post-transfections, the cells were incubated in the absence or presence of 30 μg/ml BFA for a further 4 h. The cells were then fractionated into cytosol (*C*) and membrane (*M*) fractions, equal volumes of which were resolved by SDS-PAGE and probed by immunoblotting with anti-GFP. *Panel A* shows a representative immunoblot, whereas *panel B* shows averaged data for percent palmitoylation ± S.E. of membrane-bound CSP4CL (without co-expression of DHHCs) in the absence or presence of BFA treatment ($n = 7$). *, p value of <0.0000005. Positions of molecular weight standards are shown on the *left*; the *arrowhead* denotes unpalmitoylated CSP, whereas the *asterisk* highlights palmitoylated CSP.

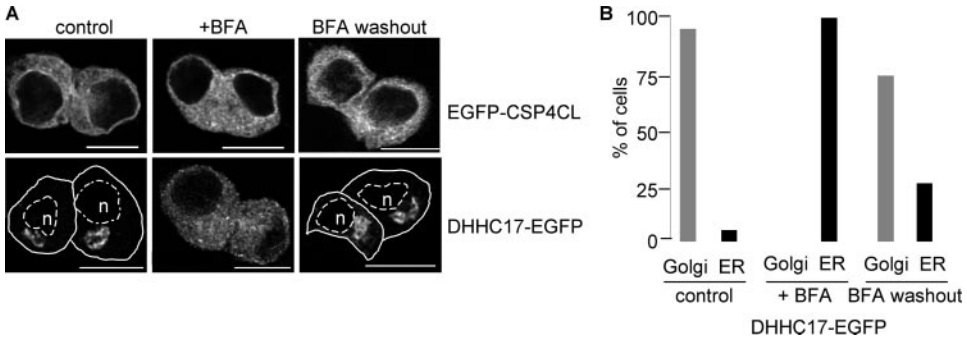

FIGURE 9. **Intracellular localization of EGFP-CSP4CL following BFA treatment and washout.** PC12 cells transfected with EGFP-CSP4CL or DHHC17-EGFP were either untreated (*control*), incubated in 30 μg/ml BFA and 10 μg/ml cycloheximide for 2 h (+*BFA*), or BFA/cycloheximide-treated and then washed and incubated in the presence of cycloheximide for 4 h (*BFA washout*). Cells were examined using a Zeiss LSM510 Axiovert laser scanning confocal microscope. For clarity, a rough outline of the cell membrane (*solid line*) and nuclei (*dashed line*, *n*) is shown for DHHC17-EGFP-expressing cells that were untreated or subjected to BFA washout. *Scale bars* represent 10 μm. *B*, DHHC17-EGFP-expressing cells under all treatments were scored for a Golgi localization or an ER (dispersed) localization. The total number of cells counted was 61 for the control condition, 50 for BFA treatment, and 74 for BFA washout.

teins with specific sub-domains of the Golgi, which facilitates interaction with CSP; and (iii) specific cofactors that regulate the CSP/DHHC interaction (16).

Based upon the work presented, we propose a model for CSP membrane binding and palmitoylation, whereby CSP utilizes a weak membrane affinity to bind transiently to cell membranes and "sample" them for DHHC content. Upon association with Golgi membranes, CSP is recognized by DHHC3/7/15/17, which catalyze the palmitoylation and stable membrane anchoring of CSP, facilitating forward transport (Fig. 10). At the heart of this model is the proposed transient membrane association of CSP. Although we do not have direct data to show reversible association of CSP with membranes, the following points are consistent with this idea as follows. (i) Specific mutations around or within the cysteine-string domain lead to stable membrane binding, consistent with the wild-type protein having an underlying membrane affinity. (ii) *In silico* analysis identified a region in CSP, including the cysteine-string domain having a propensity to move to the membrane interface but not traverse the bilayer, and experiments *in vitro* showed an association of recombinant CSP with isolated cellular membranes (25). (iii) Experiments comparing the extent of palmitoylation of wild-type CSP and CSP4CL following BFA treatment (Figs. 7 and 8) suggest that palmitoylation of wild-type CSP is rate-limited by membrane affinity. This observation is consistent with unpalmitoylated CSP having a slow membrane binding step, or a rapid dissociation from membranes. (iv) Pulse-chase experiments in PC12 cells reveal a time-dependent increase in palmitoylated CSP on membranes but very little change in the extent of unpalmitoylated CSP in the membrane fraction. These observations would be predicted if CSP was rapidly associating/dissociating from membranes and required palmitoylation for stable membrane binding (as we propose).

Concluding Remarks—The identification of DHHC3, -7, -15, and -17 as enzymes that can palmitoylate CSP and lead to its stable membrane binding suggests that there may be some redundancy in palmitoylation of DHHC substrates. Alternatively, different DHHC isoforms may palmitoylate CSP in distinct cell types and tissues. All the enzymes identified as CSP PATs display some degree of substrate specificity. DHHC17 did not palmitoylate PSD-95, GAP-43, Gα, or the γ2 subunit of $GABA_A$ (14, 40). Similarly, DHHC15 was inactive against Lck, H-Ras, and Gα and was only marginally active against the γ2 subunit of $GABA_A$ (14, 40). DHHC7 did not enhance palmitoylation of Lck or H-Ras, whereas DHHC3 was not active against Lck (14). Furthermore, many of the DHHC proteins that tested negative in our assay have previously been shown to palmitoylate specific substrates (see *e.g.* Refs. 14 and 41). Thus, there appears to be a good degree of specificity exhibited by the DHHC proteins that palmitoylate CSP. At present we do not know how CSP/DHHC specificity is regulated, but some possibilities include: (i) specific structural features of the DHHC region and/or other domains of DHHC3/7/15/17 regulating interaction with CSP; (ii) the association of these DHHC pro-

Analyses of CSP truncation mutants highlighted a key role for a lysine-proline-lysine motif immediately downstream of the membrane-binding domain (Fig. 4). This motif weakens membrane affinity of truncation mutants and at the same time facilitates efficient palmitoylation. Interestingly, mutation of this domain in full-length CSP did not lead to accumulation of unpalmitoylated CSP on membranes (supplemental Fig. S2), implying that the intact C terminus of full-length CSP (which is highly charged) can regulate membrane association in the absence of the KPK motif. Nevertheless, this amino acid triplet

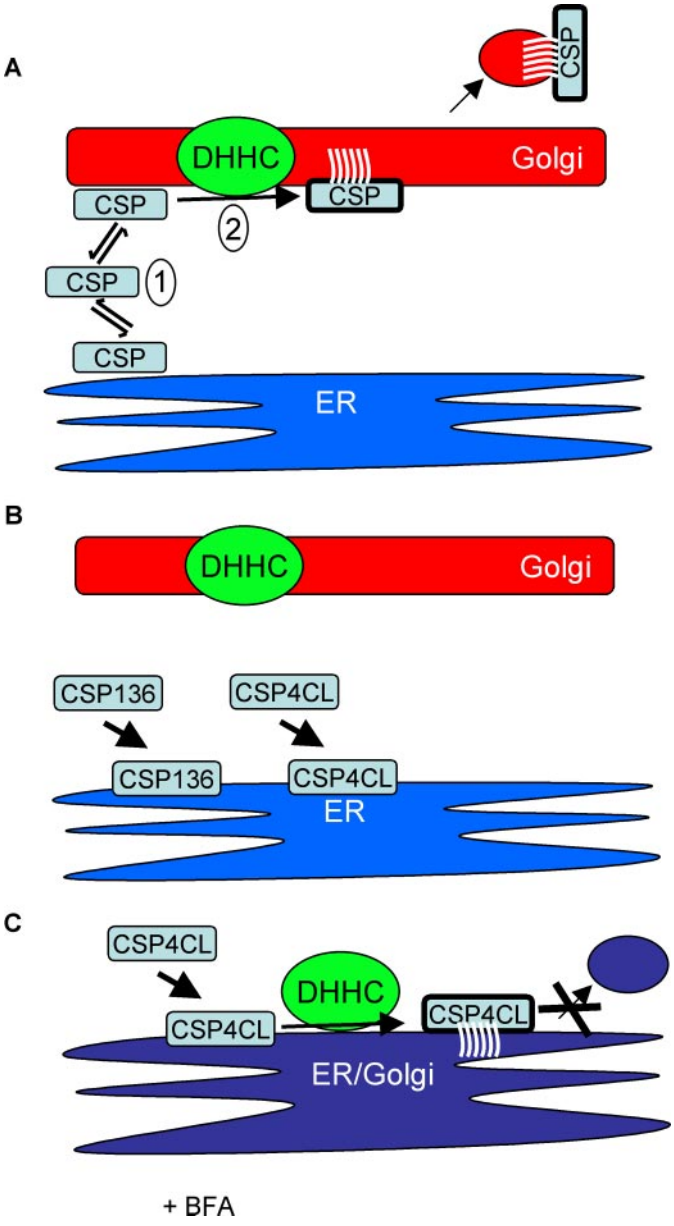

FIGURE 10. **Membrane binding and palmitoylation of CSP.** *A*, CSP utilizes a weak membrane affinity to sample intracellular membranes (*1*). Upon binding to Golgi membranes, CSP is recognized and palmitoylated by its partner DHHC proteins (*2*). Palmitoylation leads to stable membrane binding of CSP and may facilitate forward transport. *B*, the enhanced membrane affinity of CSP136 and CSP4CL leads to tight binding to the most abundant cellular membranes, such as the ER, and physical separation from Golgi-localized DHHC proteins. *C*, BFA treatment induces the fusion of ER and Golgi membranes and puts CSP4CL and DHHC proteins on the same membrane compartment. This membrane mixing allows palmitoylation of CSP4CL but is not sufficient to allow transport out of the ER.

is clearly important for palmitoylation of full-length CSP, perhaps regulating the affinity of DHHC interaction (see supplemental Fig. S2 and reference 24). One possibility that we wanted to exclude was that the loss of tight membrane binding of CSP136 following addition of KPK (Fig. 4) did not simply occur due to the addition of *any* amino acids downstream of the cysteine string. To test this, we introduced a K137A mutation into a CSP143 mutant (supplemental Fig. S2). Replacement of Lys^{137} in this mutant promoted a large increase in membrane binding and similarly a decreased palmitoylation. Thus, we can conclude: (i) the KPK motif is essential for palmitoylation of CSP; (ii) this motif affects the membrane interaction of CSP (mutants); and (iii) residues between amino acids 144–198 are also important for weakening membrane affinity of CSP and are sufficient in this regard following removal of the KPK motif.

The role of palmitoylation in regulating protein sorting is an emerging area of cell biology (3). Although palmitoylation of CSP is essential for sorting of CSP, it is not clear whether palmitoylation plays an active role in this process (for example by driving association of CSP with budding vesicles) or an indirect role (by promoting stable membrane attachment and thus allowing other domains of CSP to facilitate sorting). Whatever the mechanism, our experiments examining CSP4CL localization following BFA washout (Fig. 9) suggest that palmitoylation of CSP can be uncoupled from forward transport in the secretory pathway. It is formally possible that loss of specific palmitoylated cysteines in the CSP4CL mutant directly inhibits traffic from the ER (*i.e.* that CSP needs to be fully palmitoylated to traffic). This is unlikely given that we have previously shown that other CSP mutants lacking 3–4 cysteines (and hence palmitoylation sites) traffic similarly to wild-type protein (24). Thus, we favor the view that forward traffic of palmitoylated CSP is linked to palmitoylation at a specific cell location (*i.e.* the Golgi) and that factors required for CSP sorting are not present at the ER following BFA washout.

The results of this study are reminiscent of recent work studying palmitoylation and trafficking of H- and N-Ras (6, 7). Farnesylation of these proteins provides a weak membrane affinity (42, 43). This initial membrane interaction is weak and presumed to allow Ras to associate with any intracellular membrane. Because the Ras palmitoyl transferase, DHHC9, is localized to ER/Golgi membranes (16), palmitoylation only occurs on these membranes, probably allowing access of Ras to the secretory pathway and facilitating its forward transport to the plasma membrane (6, 7). Our results suggest that membrane sampling through transient membrane interactions is not restricted to lipidated (prenylated or myristoylated) proteins but may also occur via specialized protein domains, such as the cysteine-string domain of CSP.

Acknowledgments—We are very grateful to Rory Duncan and Colin Rickman (University of Edinburgh) for advice and help with confocal imaging analysis. The DHHC17-EGFP plasmid was provided by Alaa El-Husseini.

REFERENCES

1. Resh, M. D. (2006) *Nat. Chem. Biol.* **2,** 584–590
2. Linder, M. E., and Deschenes, R. J. (2007) *Nat. Rev. Mol. Cell Biol.* **8,** 74–84
3. Greaves, J., and Chamberlain, L. H. (2007) *J. Cell Biol.* **176,** 249–254
4. Nadolski, M. J., and Linder, M. E. (2007) *FEBS J.* **274,** 5202–5210
5. Hayashi, T., Rumbaugh, G., and Huganir, R. L. (2005) *Neuron* **47,** 709–723
6. Goodwin, J. S., Drake, K. R., Rogers, C., Wright, L., Lippincott-Schwartz, J., Philips, M. R., and Kenworthy, A. K. (2005) *J. Cell Biol.* **170,** 261–272
7. Rocks, O., Peyker, A., Kahms, M., Verveer, P. J., Koerner, C., Lumbierres, M., Kuhlmann, J., Waldmann, H., Wittinghofer, A., and Bastiaens, P. I. H. (2005) *Science* **307,** 1746–1752
8. Salaun, C., Gould, G. W., and Chamberlain, L. H. (2005) *J. Biol. Chem.* **280,** 1236–1240
9. Roy, S., Plowman, S., Rotblat, B., Prior, I. A., Muncke, C., Grainger, S.,

Parton, R. G., Henis, Y. I., Kloog, Y., and Hancock, J. F. (2005) *Mol. Cell Biol.* **25,** 6722–6733
10. Lobo, S., Greentree, W. K., Linder, M. E., and Deschenes, R. J. (2002) *J. Biol. Chem.* **277,** 41268–41273
11. Roth, A. F., Feng, Y., Chen, L., and Davis, N. G. (2002) *J. Cell Biol.* **159,** 23–28
12. Roth, A. F., Wan, J., Bailey, A. O., Sun, B., Kuchar, J. A., Green, W. N., Phinney, B. S., Yates III, J. R., and Davis, N. G. (2006) *Cell* **125,** 1003–1013
13. Keller, C. A., Yuan, X., Panzanelli, P., Martin, M. L., Alldred, M., Sassoe-Pognetto, M., and Luscher, B. (2004) *J. Neurosci.* **24,** 5881–5891
14. Fukata, M., Fukata, Y., Adesnik, H., Nicoll, R. A., and Bredt, D. S. (2004) *Neuron* **44,** 987–996
15. Huang, K., Yanai, A., Kang, R., Arstikaitis, P., Singaraja, R. R., Metzler, M., Mullard, A., Haigh, B., Gauthier-Campbell, C., and Gutekunst, C.-A. (2004) *Neuron* **44,** 977–986
16. Swarthout, J. T., Lobo, S., Farh, L., Croke, M. R., Greentree, W. K., Deschenes, R. J., and Linder, M. E. (2005) *J. Biol. Chem.* **280,** 31141–31148
17. Politis, E. G., Roth, A. F., and Davis, N. G. (2005) *J. Biol. Chem.* **280,** 10156–10163
18. Zinsmaier, K. E., Eberle, K. K., Buchner, E., Walter, N., and Benzer, S. (1994) *Science* **263,** 977–980
19. Umbach, J. A., Zinsmaier, K. E., Eberle, K. K., Buchner, E., Benzer, S., and Gundersen, C. B. (1994) *Neuron* **13,** 899–907
20. Zhang, H., Kelley, W. L., Chamberlain, L. H., Burgoyne, R. D., Wollheim, C. B., and Lang, J. (1998) *FEBS Lett.* **437,** 267–272
21. Chamberlain, L. H., and Burgoyne, R. D. (1998) *Mol. Biol. Cell* **9,** 2259–2267
22. Fernandez-Chacon, R., Wolfel, M., Nishimune, H., Tabares, L., Schmitz, F., Castellano-Munoz, M., Rosenmund, C., Montesinos, M. L., Sanes, J. R., Schneggenburger, R., and Sudhof, T. C. (2004) *Neuron* **42,** 237–251
23. Gundersen, C. B., Mastrogiacomo, A., Faull, K., and Umbach, J. A. (1994) *J. Biol. Chem.* **269,** 19197–19199
24. Greaves, J., and Chamberlain, L. H. (2006) *Mol. Biol. Cell* **17,** 4748–4759
25. Boal, F., Le Pevelen, S., Cziepluch, C., Scotti, P., and Lang, J. (2007) *Biochim. Biophys. Acta* **1773,** 109–119
26. Stowers, R. S., and Isacoff, E. Y. (2007) *J. Neurosci.* **27,** 12874–12883
27. Ohyama, T., Verstreken, P., Ly, C. V., Rosenmund, T., Rajan, A., Tien, A.-C., Haueter, C., Schulze, K. L., and Bellen, H. J. (2007) *J. Cell Biol.* **179,** 1481–1496
28. Chamberlain, L. H., and Burgoyne, R. D. (1996) *J. Biol. Chem.* **271,** 7320–7323
29. Coppola, T., and Gundersen, C. (1996) *FEBS Lett.* **391,** 269–272
30. Eberle, K. K., Zinsmaier, K. E., Buchner, S., Gruhn, M., Jenni, M., Arnold, C., Leibold, C., Reisch, D., Walter, N., Hafen, E., Hofbauer, A., Pflugfelder, G. O., and Buchner, E. (1998) *Cell Tissue Res.* **294,** 203–217
31. van de Goor, J., and Kelly, R. B. (1996) *FEBS Lett.* **380,** 251–256
32. Chamberlain, L. H., and Burgoyne, R. D. (1998) *Biochem. J.* **335,** 205–209
33. Mastrogiacomo, A., Kohan, S. A., Whitelegge, J. P., and Gundersen, C. B. (1998) *FEBS Lett.* **436,** 85–91
34. Chamberlain, L., Graham, M., Kane, S., Jackson, J., Maier, V., Burgoyne, R., and Gould, G. (2001) *J. Cell Sci.* **114,** 445–455
35. Ohno, Y., Kihara, A., Sano, T., and Igarashi, Y. (2006) *Biochim. Biophys. Acta* **1761,** 474–483
36. Donaldson, J. G., Kahn, R. A., Lippincott-Schwartz, J., and Klausner, R. D. (1991) *Science* **254,** 1197–1199
37. Lippincott-Schwartz, J., Yuan, L. C., Bonifacino, J. S., and Klausner, R. D. (1989) *Cell* **56,** 801–813
38. Gonzalo, S., and Linder, M. E. (1998) *Mol. Biol. Cell* **9,** 585–597
39. Lippincott-Schwartz, J., Donaldson, J. G., Schweizer, A., Berger, E. G., Hauri, H.-P., Yuan, L. C., and Klausner, R. D. (1990) *Cell* **60,** 821–836
40. Fang, C., Deng, L., Keller, C. A., Fukata, M., Fukata, Y., Chen, G., and Luscher, B. (2006) *J. Neurosci.* **26,** 12758–12768
41. Fernandez-Hernando, C., Fukata, M., Bernatchez, P. N., Fukata, Y., Lin, M. I., Bredt, D. S., and Sessa, W. C. (2006) *J. Cell Biol.* **174,** 369–377
42. Shahinian, S., and Silvius, J. (1995) *Biochemistry* **34,** 3813–3822
43. Magee, A. I., Gutierrez, L., McKay, I. A., Marshall, C. J., and Hall, A. (1987) *EMBO J.* **6,** 3353–3357